

https://dspace.org/

Evaluating Satellite Precipitation Products in Capturing the Spatiotemporal Rainfall Variability Across North Darfur State Sudan

M Altoom; Elhadi Adam; K Ali; Colbert Jackson

https://hdl.handle.net/10539/46519
SCOPUS

Downloaded from a DSpace repository. https://dspace.org/

Remote Sensing in Earth Systems Sciences (2025) 8:753–771
https://doi.org/10.1007/s41976-025-00219-2

RESEARCH

Evaluating Satellite Precipitation Products in Capturing the Spatio-temporal Rainfall Variability Across North Darfur State, Sudan

Mohammed B. Altoom[1,4] · Elhadi Adam[1] · Khalid Adem Ali[1,2] · Colbert M. Jackson[1,3]

Received: 12 January 2024 / Revised: 17 October 2024 / Accepted: 18 March 2025 / Published online: 9 April 2025
© The Author(s) 2025

Abstract
Accurate rainfall measurement is vital when investigating spatio-temporal precipitation variability, especially in arid lands. However, there are regions worldwide where only a few ground-based observations are made. This research evaluated the applicability of six satellite precipitation products (SPPs) in detecting rainfall variability in North Darfur State, Sudan. The SPPs were Tropical Rainfall Measuring Mission (TRMM) Multi-satellite Precipitation Analysis (TMPA), African Rainfall Climatology (ARC), Climate Hazards Group Infrared Precipitation with Station Data (CHIRPS), Integrated Multi-satellitE Retrievals for Global Precipitation Measurements (GPM) Final Run (GPMIMERG), Precipitation Estimation from Remote Sensing Information using Artificial Neural Networks-Climate Data Record (PERSIANN-CDR), and the Tropical Applications of Meteorology using SATellite and ground-based observations (TAMSAT). The SPPs were assessed at daily, monthly, and annual timescales for 2000–2019. Four categorical indices, i.e., the probability of detection (POD), probability of false alarm (POFA), bias in detection (BID) and Heidke skill score (HSS), and four continuous indices, i.e., the Pearson correlation coefficient (r), the root mean square error (RMSE), the per cent bias (Pbias), and the Nash–Sutcliffe model efficiency coefficient (NSE) were used to evaluate the accuracy of the SPPs. Results of the statistical analysis showed that (1) at the daily timescale, the SPPs underestimate daily rainfall by 6.53–17.61%, and CHIRPS was the best for detecting rainy days, while PERSIANN-CDR performed poorly; (2) monthly and annual scales performed better than daily timescale, and TAMSAT and CHIRPS portrayed better performance than the other SPPs. Therefore, the two could reasonably estimate rainfall amounts in North Darfur State.

Keywords ARC · CHIRPS · GPMIMERG · PERSIANN-CDR · TMPA · TAMSAT · North Darfur State

1 Introduction

Rainfall is vital to how water moves through Earth's water cycle, which connects the land, atmosphere and oceans [1]. Therefore, rainfall is essential in Earth's climate system [2, 3]. Rainfall is not evenly distributed worldwide—some places receive more than normal, while others become prone to droughts [4]. The variable distribution, rate and amount of rainfall determines Earth's ecosystems [5, 6]. Reliable measurement of rainfall data is essential for understanding the spatio-temporal variability

✉ Mohammed B. Altoom
mohbasharadam@gmail.com; altoomm@ukzn.ac.za

Elhadi Adam
elhadi.adam@wits.ac.za

Khalid Adem Ali
alika@cofc.edu

Colbert M. Jackson
Jackson.C@ufs.ac.za

[1] Faculty of Science, School of Geography, Archaeology and Environmental Studies, University of the Witwatersrand, Johannesburg 2050, South Africa

[2] Department of Geology and Environmental Geosciences, College of Charleston, Charleston, SC 29424, USA

[3] Department of Geography, Faculty of Natural and Agricultural Sciences, University of the Free State, Bloemfontein 9300, South Africa

[4] School of Agricultural, Earth and Environmental Sciences, University of KwaZulu-Natal, Westville Campus, Durban 4000, South Africa

of rainfall at various timescales and its effects on hydrology, agriculture, and ecosystem functioning [6–8]. Traditionally, rain gauge observations have been used to characterize the spatio-temporal variability of rainfall [9]. However, in developing countries, due to various reasons, rainfall data is often unavailable, and even if it does exist, the quality are poor or inaccessible [10]. For example, the Meteorological Department of Sudan does not receive sufficient funding from the government; this has hampered the recruitment and retention of trained and volunteer observers and the ability to rehabilitate malfunctioned and/or abandoned meteorological stations [11, 12]. In addition, the second Sudanese Civil War between 1983 and 2005 interfered with measuring and reporting meteorological data, especially in the southern region [13–15]. Therefore, political unrest and conflict significantly influenced the distribution, density and quality of rain gauge measurements. It is particularly true in the Darfur region, which often shows gaps in temporal rainfall data [12, 16].

The limitations associated with rain gauge observations have necessitated alternative methods to measure rainfall [4]. Fortunately, remote sensing provides an alternative approach to ground-based rainfall measurement and monitoring methods. Rainfall data can be gathered from satellite-based products [6]. A variety of satellite precipitation products (SPPs) are produced by the passive microwave (PMW)- and thermal infrared radiation (TIR)-based sensors onboard both geostationary and LEO satellites. The TIR-based method uses algorithms to assess rainfall from cloud-top temperature [17]. The PMW technique can penetrate clouds and produce accurate rainfall amounts compared to the TIR-based technique, which has difficulties identifying rain-producing clouds [18, 19]. However, the poor temporal resolution of low Earth-orbiting satellites makes the PMW technique not helpful in assessing accumulated rainfall over a longer duration [20]. Therefore, uncertainties may originate from the temporal resolutions of satellites, the algorithms used to assess rainfall from cloud-top temperature, and satellite instruments themselves—these reduce the accuracy of satellite rainfall estimates [21]. Other techniques, e.g., combined PMW/TIR [22] or merged PMW/TIR technique with rain gauge observations or numerical weather models [23] were developed to improve the accuracy of satellite rainfall assessment. Several studies, e.g., Huffman et al. [24], Xie and Arkin [25], Boushaki et al. [26], Ebert et al. [27], Katiraie-Boroujerdy et al.[28], Sanogo et al. [29], Dezfuli et al. [30], Bai et al. [31], Dembélé and Zwart [32], and Ayugi et al. [33] have been conducted using the latter technique at different spatial and temporal scales.

The SPPs play a vital role in accurately mapping the spatiotemporal variability of rainfall, which is essential in designing climate change adaptation strategies. Sanogo et al. [29] evaluated the spatio-temporal characteristics of rainfall in West Africa using the gridded African Rainfall Climatology Version 2 (ARC 2.0). The results were consistent with ground observation data. Dezfuli et al. [30] showed that the diurnal precipitation cycle was better captured by the Integrated Multi-satellitE Retrievals for Global Precipitation Measurement (IMERG)-Final v6 (IMERG6) than the TRMM (Tropical Rainfall Measuring Mission) Multi-satellite Precipitation Analysis (TMPA), and the products exhibited a better agreement with ground data in dry East and humid West Africa than with the southern Sahel. The Usman et al. [23] analysis assessed the capability of four satellite-based rainfall models, i.e., TAMSAT (Tropical Applications of Meteorology using SATellite) African Rainfall Climatology and Time series (TARCAT), ARC 2.0, TRMM, and Climate Hazards group Infrared Precipitation with Stations (CHIRPS) to portray rainfall trends in West Africa. Additionally, Dembélé and Zwart [32] evaluated how well the TRMM, ARC 2.0, CHIRPS 2.0, Precipitation Estimation from Remote Sensing Information using artificial neural networks (PERSIANN), African Rainfall Estimation (RFE 2.0), TAMSAT, and TAR CAT performed at estimating rainfall amounts in the semi-arid Sahelian region of Burkina Faso. The satellites performed poorly at daily time scales but better at annual timescales, with the best product being the RFE 2.0. The CHIRPS 2.0 and TARCAT were the best products for assessing drought in the Upper Blue Nile Basin, Ethiopia, according to Bayissa et al. [34]—the study compared the capabilities of five satellite precipitation products, i.e., ARC 2.0, CHIRPS 2.0, PERSIANN, TARCAT 2.0, and TMPA. Toté et al. [20] analyzed three satellite rainfall estimates, i.e., TARCAT 2.0, Famine Early Warning System NET work (FEWS NET), RFE 2.0, and CHIRPS 2.0 for drought and flood monitoring in tropical climate areas of Mozambique—TARCAT 2.0 was superior at modelling the relative frequency of rainfall events. Ahmed et al. [35] evaluated TRMM and RFE 2.0 over the Sudanese portion of the Blue Nile River and found that the TRMM product performance was superior to RFE 2.0. Girm [36] explored TAMSAT 3.1 over southern Ethiopia and demonstrated that TAMSAT matched rain gauge data. Lu et al. [37] evaluated the SPPs in analyzing changes in rainfall patterns in Namibia and found that the TMPA estimations and the data from the rain gauges agreed at monthly and annual timescales. Babaousmail et al. [38] showed that the National Oceanic and Atmospheric Administration (NOAA) Climate Prediction Center Morphing Technique (CMORPH) was the most suitable product for satellite-based precipitation estimates for the prevailing Mediterranean climate. However, the majority of the aforementioned studies demonstrated that the algorithm performance varies significantly depending on topography, location, season, and local climate [13, 20, 23, 39].

The Darfur region is characterized by spatial and temporal rainfall variability. The variability aggravates the problem of limited soil productivity and the spatial distribution of agricultural land. Despite these challenges, 80–90% of the population relies on rainfed agriculture and livestock rearing as their

main sources of income [40, 41]. Therefore, climate-related hazards, e.g., drought, have severe and disproportionate effects, especially on the rural poor, because crop yields are unpredictable and difficult to anticipate. The Sahel region's devastating droughts and hunger in the 1970s, 1980s, and mid-1990s, particularly in Chad and Sudan's Darfur region, occasionally led to violent clashes between nomadic tribes and local farmers [42]. Therefore, understanding the spatio-temporal variation in rainfall, especially in arid and semi-arid regions is critical for predicting extreme hydrological events and mitigating climate-related risks through improved water resources planning, agricultural development of agro-pastoral systems, and environmental management and restoration [43].

Hydrological modeling for water management in arid lands requires accurate spatio-temporal rainfall measurements. However, mostly, only a few ground-based observations are available. Therefore, SPPs can fill the spatial and temporal rainfall data gaps in such regions. Satellite precipitation products have performed differently in mapping the spatio-temporal variability of rainfall. Hence, accurately detecting rainfall variability and trends has been challenging. This study aimed to determine whether it is feasible to estimate rainfall variability across North Darfur State at daily, monthly, and annual timescales using SPPs to inform decisions in water management. No relevant studies have been conducted in the North Darfur State. The SPPs used were the TRMM (Tropical Rainfall Measuring Mission) Multi-satellite Precipitation Analysis (TMPA), African Rainfall Climatology (ARC), Climate Hazards group Infrared Precipitation with Stations (CHIRPS), Integrated Multi-satellitE Retrievals for Global Precipitation Measurements (GPM) Final Run (GPMIMERG), Precipitation Estimation from remote sensing information using artificial neural networks-Climate Data Record (PERSIANN-CDR), and Tropical Applications of Meteorology using SATellite and ground-based observations (TAMSAT).

2 Materials and Methods

2.1 The Study Area

The study area is located in North Darfur State, in western Sudan, at latitude 11° 45′ 49″ to 20° 00′ 30″ N and longitude 22° 46′ 47″ to 27° 29′ 47″ E (Fig.Fig. 1). The southern part of North Darfur state comprises a higher concentration of population and economic activities. The Jabbed Marrah Mountains, roughly at 3000 m above sea level, are at the maximum elevation within the study area [40, 44]. The region is mainly arid and semi-arid, with great geographical and temporal variability in rainfall. Most rainfall of North Darfur comes from south-westerly winds and the rainy season is mainly from June to October, with average annual rainfall ranging between 152 mm yr^{-1} in the northern parts and 540 mm yr^{-1} in the southern parts and the rainfall is at its peak in August [12, 16]. In Sudan, the rainy season often consists of many dry days and a few heavy but short rainstorms. The few rainy days may take the following forms: (i) rain may start early, followed by partial/complete failure, (ii) rain may start late, (iii) the few rainy days may spread throughout the wet season, and (iv) evenly distributed but infrequent heavy rainfall. Yearly mean maximum and mean minimum temperatures are 42 °C and 11 °C respectively [45].

The largest food crop is millet, grown in sandy soil (qoz) [46, 47]. Agriculture is constrained by poor soil fertility, small per capita landholding, soil degradation, and erratic rainfall; as a result, most parts of the area are chronically food insecure [40].

2.2 Datasets

2.2.1 In Situ Rainfall Data

Daily rainfall data from 11 rainfall stations in North Darfur State were obtained from the Ministry of Agriculture for the period from 2000 to 2009 (Fig. Figure 1). The rainfall stations in the study area are located in densely populated areas in south-western parts, especially in areas of intense agricultural activity, because the northern part of the study area is mostly desert [12, 45]. Only less than 10% of rainfall data were missing at each of the 11 weather stations considered in this study [9, 48, 49]. A brief description of the 11 rainfall stations is presented in Table 1. The stations, installed at different elevations, have been recording data since 1970.

2.2.2 Satellite-based Precipitation Products

Six satellite-based precipitation products (SPPs) were compared against rain gauge observations to evaluate their efficiency in capturing rainfall variability across North Darfur State for 20 years, i.e., from 2000 to 2019. The SPPs used were the Tropical Rainfall Measuring Mission-based (TRMM) Multi-Satellite Precipitation Analysis (TMPA-3B42 7.0), African Rainfall Climatology Version 2 (ARC 2.0), Climate Hazards Group Infrared Precipitation with Stations Data (CHIRPS 2.0), Global Precipitation Measurements (GPM)—the Integrated Multi-satellitE Retrievals Final Runv6 (GPMIMERG 6.0), Precipitation Estimation from remote sensing information using artificial neural networks-Climate Data Record (PERSIANN-CDR), and the Tropical Applications of Meteorological using SaTEllite and ground-based observations (TAMSAT 3.1). The parameters of the six SPPs are shown in Table 2.

The TRMM-based TMPA provides quasi-global precipitation products for the years 1998 to 2019 with a spatial resolution of $0.25° \times 0.25°$ and a temporal resolution of daily and three hours, covering the latitudes 50° N–50° S [2,

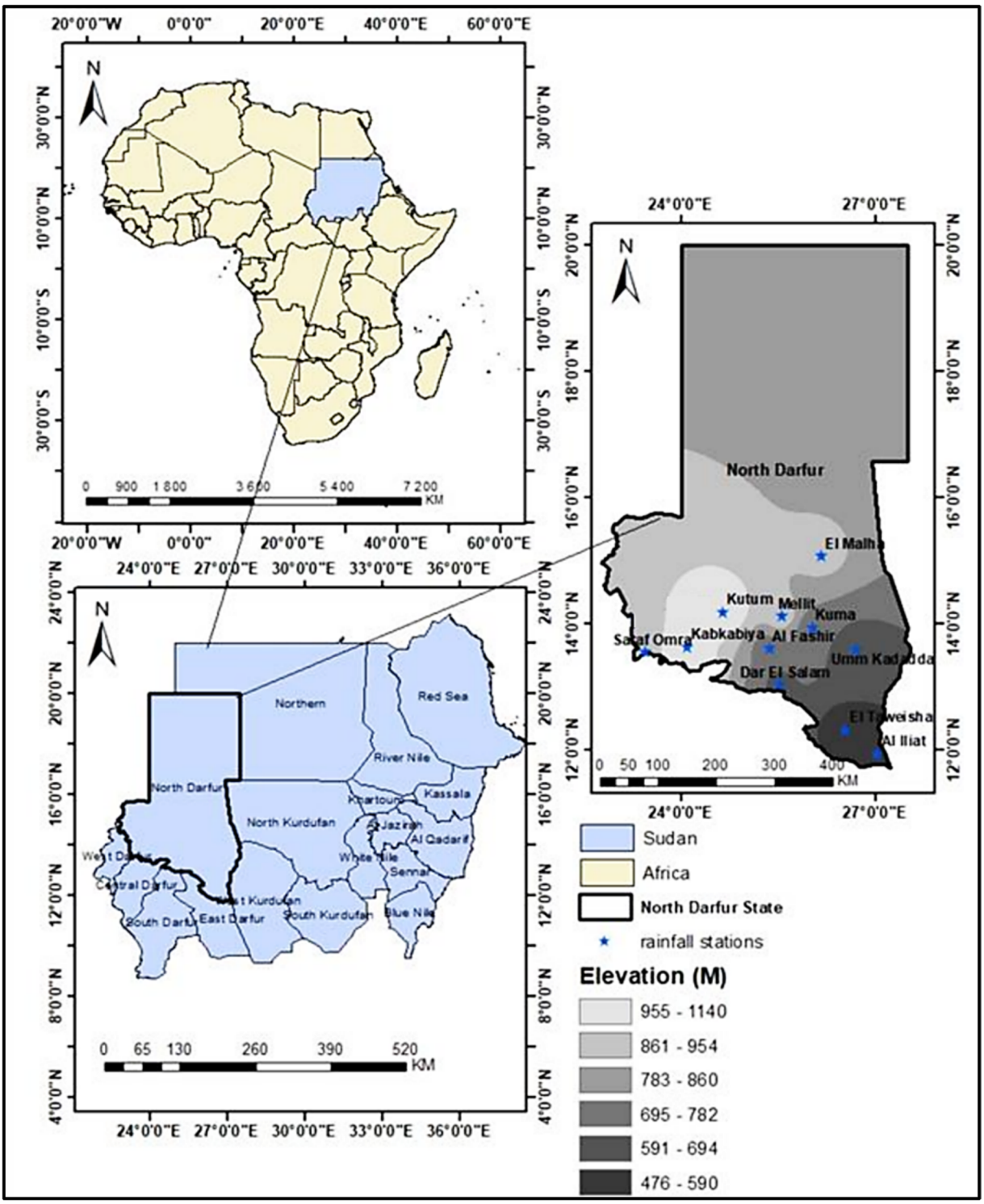


Fig. 1 Map of the study area in North Darfur State in Sudan; the star symbol shows locations of the rainfall stations

50, 51]. The TMPA is combined into gauge-adjusted daily (3B42) and monthly (3B43) post-real-time precipitation. Only the daily rainfall dataset was downloaded, and TMPA version 7 used (TMPA-3B42 7.0). The TMPA product was accessed at https://disc.gsfc.nasa.gov/. The ARC 2.0 data have been available as daily gridded precipitation data centered over the African continent at a spatial resolution of 10 km (0.1°) since 1983. The ARC 2.0 was developed by the

Table 1 Characteristics of the 11 rainfall stations in North Darfur State for the study period 2000–2019

No	Station name	Latitude (°N)	Longitude (°E)	Elevation (amsl)	Data availability	Mean annual rainfall (mm)
1	Al Fashir	13° 38'	25° 20'	0740	Daily	232.3
2	Al Liait	11° 57'	27° 04'	0587	Daily	517.1
3	Dar El Salam	13° 05'	25° 53'	0817	Daily	302.2
4	El Malha	15° 09'	26° 15'	0900	Daily	211.7
5	El Tawiesha	12° 29'	26° 59'	0591	Daily	363.4
6	Kabkabiya	13° 39'	24° 5'	1120	Daily	558.6
7	Kuma	13° 39'	26° 01'	0875	Daily	220.2
8	Kutum	14° 21'	24° 40'	1160	Daily	279.8
9	Mellit	14° 13'	25° 55'	0900	Daily	223.9
10	Saraf Omra	13° 47'	23° 30'	1105	Daily	404.3
11	Umm Kadadda	13° 59'	26° 14'	0595	Daily	227.2

Table 2 Parameters of the satellite-based precipitation products (SPPs) used in the study for the period 2000–2019;

No	Satellites-based rainfall products	Sensor	Temporal coverage	Spatial coverage	Temporal resolution	Spatial resolution
1	TMPA-3B42 7.0	TIR/PMW	1998–2019	Near global	Daily	0.25°×0.25°
2	ARC 2.0	TIR	1983–present	Africa	Daily	0.1°×0.1°
3	CHIRPS 2.0	TIR	1981–present	Near global	Daily	0.05°×0.05°
4	GPMIMERG 6.0	TIR/PMW	2000–2019	Near global	Daily	0.1°×0.1°
5	PERSIANN-CDR	TIR	1982–2020	Near global	Daily	0.25°×0.25°
6	TAMSAT 3.1	TIR	1983–present	Africa	Daily	0.0375°×0.0375°

TIR thermal infrared, *PMW* passive microwave.

Climate Prediction Center of the NOAA. ARC 2.0 data were retrieved from the European Organization for the Exploitation of Meteorological Satellites (EUMETSAT), which provides 3-hourly geostationary thermal infrared (TIR) data, and the Global Telecommunication System (GTS) gauge measurements reporting 24-h rainfall accumulations over Africa. Both the EUMETSAT and GTS have high quality data [23, 52]. The daily ARC 2.0 rainfall estimates for the period were retrieved from https://www.icpac.net/data-center/arc2/. The CHIRPS Version 2.0 rainfall dataset was developed by the United States Geological Survey in collaboration with the Climate Hazard Group at the University of California. These data are available from 1981 onwards and span 50° N–50° S (all longitudes included). To create gridded rainfall time series, CHIRPS incorporates the Climate Hazard group Precipitation climatology (CHPclim) that incorporates (i) satellite information to represent sparsely gauged locations, (ii) 0.05° resolution cold cloud duration (CCD)-based Climate Hazard group Infrared Precipitation (CHIRP) estimates, and (iii) rain gauge data [53]. For this study, daily CHIRPS2.0 datasets from 2000 to 2019 were used as obtained from https://earlywarning.usgs.gov/. The GPMIMERG 6.0 has a spatial resolution of (0.1°×0.1°) and a temporal resolution of half an hour. The Global Precipitation Climatology Center's (GPCC) monthly gauge analysis is used to calibrate the Integrated Multi-satellitE Retrievals for GPM (IMERG), which is produced using combined passive microwave (PMW) and infrared (IR) data from the GPM constellation [54, 55]. The most recent version of GPM (IMERG) is Final Run v 6B (IMERG6), which covers Early Run (near real-time with a latency of 6 h), Late Run (near real-time with a latency of 18 h), and Final Run (gauge-adjusted with a delay of four months) [2, 55]. In this study, daily IMERG6 were obtained from https://gpm.nasa.gov/data/. The PERSIANN climate database was created by scientists from the University of California's Center for Remote Sensing and Hydrometeorology [56]. The PERSIANN product applies the artificial neural network (ANN) model to convert IR information into rain rates [57]. For this study, daily PERSIANN data were downloaded from https://climatedataguide.ucar.edu. The TAMSAT algorithm, based on Meteosat thermal infrared (TIR) from EUMESTAT [32], was developed at the University of Reading; the purpose is to estimate rainfall during drought in Africa and to provide famine warnings. TAMSAT's rainfall estimation is based on the assumption of a positive linear relationship between the lifetime of convective clouds and rainfall amount at the surface. Therefore, TAMSAT works best for convective precipitation [58–60]. Since 1982, TAMSAT products have been provided with a spatial resolution of 0.0375° and temporal

resolutions of decadal, seasonal, and monthly intervals [6]. In this study, daily TAMSAT data for the period 2000–2019 were obtained from https://www.tamsat.org.uk.

2.3 Methods

2.3.1 Evaluation of Satellite Products

The study focused on evaluating the performance of six SPPs—the TMPA 3B42/3B43-7.0, CHIRPS 2.0, PERSIANN-CDR, GPMIMERG 6.0, ARC 2.0, and TAMSAT 3.1, to identify the best products for capturing rainy days and estimating rainfall amounts and variability trends across the study area. This was done by comparing satellite products against rain gauge measurements for the 2000–2019 period at daily, monthly, and annual timescales. The point values from pixels of respective SPPs were georeferenced to gauge location and extracted from the downloaded raster files [61]. The study employed a point-to-pixel pairwise comparison approach, in which rainfall estimations from each satellite are created and compared with the data from each rain gauge [2, 6].

2.3.2 Validation Statistics

The ability of SPPs to detect rainy days, defined here as days with rainfall totaling more than 0.2 mm, was assessed based on a contingency table (Table .

Table 3 Contingency table for comparing rain gauge measurements and satellite-based rainfall estimates

	Gauge ≥ 0.2 mm	Gauge < 0.2 mm
Satellite ≥ 0.2 mm	Hits (H)	False alarm (F)
Satellites < 0.2 mm	Miss (M)	Correct no rain (D)

Table 3) using categorical statistical indices (Eqs. 1–4, Table 4). The categorical statistics used in this study were the probability of detection (POD, i.e., the proportion of observed rain days that were detected by the satellite product); the probability of false alarm (POFA, i.e., the proportion of satellite-estimated rain days that did not in fact occur); bias in detection (BID, i.e., assesses whether SPPs overestimates or underestimates rainy day frequency); and Heidke skill score (HSS, i.e., the measure of the overall skill of the rainfall-day estimates accounting for matches owing to chance) [18, 36, 61].

The performance of the SPPs in estimating the amount and variability of rainfall across the study area was also evaluated using continuous statistical indices (Eqs. 5–8). One of these indices used in this study is the Pearson correlation coefficient (r), which is used to assess the correlation's goodness of fit, with a value of 1 being the perfect score [32]. The root mean square error (RMSE) measures the mean difference between two variables; a low RMSE value indicates the predictions are precise [6, 23, 32]. The percent bias (Pbias) is used to show how well the satellite rainfall estimates correspond with the gauge rainfall data average; a positive Pbias indicates overestimates, while negative Pbias indicates underestimates. The Nash–Sutcliffe efficiency (NSE) coefficient assesses the predictive skill of models—higher values suggest a better agreement between observations and satellite estimates [62]. A negative NSE value shows that the observed mean is a better estimator than the model, while a value of zero shows that the model predictions are as accurate as the mean of the observed data [61, 63]. The test–retest reliability was used to assess the consistency and reproducibility of the results obtained.

G gauge rainfall amount, $\overline{G}$ average gauge rainfall amount, S satellite rainfall estimates, $\overline{S}$ average satellite rainfall estimate, N number of data pairs, H number of precipitation events detected by both satellites and a rain gauge, M number of precipitation events detected by a rain gauge by

Table 4 Statistical indices for satellite-based precipitation products (SPPs)

Statistics indicator	Abbreviation	Formula	Values range	Perfect score
Probability of detection	POD	$\frac{H}{H+M}$ (1)	[0, 1]	1
Probability of false alarm	POFA	$\frac{F}{H+F}$ (2)	[0, 1]	0
Bias in detection	BID	$\frac{H+F}{H+M}$ (3)	$[-\infty, +\infty]$	1
Heidke skill score	HSS	$\frac{2(HD-FH)}{(H+M)(M+D)+(H+F)(F+D)}$ (4)	(4) [- ∞, 1)	1
Pearson correlation coefficient	r	$\frac{\Sigma\left(G-\overline{G}\right)\left(S-\overline{S}\right)}{\sqrt{\Sigma\left((G-\overline{G}\right)^2\left((S-\overline{S}\right)^2}}$ (5)	[−1, 1]	1
Root mean square error	RMSE (mm)	$\sqrt{\frac{1}{N}\sum_{i=1}^{n}(S-G)^2}$ (6)	$[0, +\infty]$	0
Percent bias	Pbias (%)	$\frac{1}{N}\left(\frac{\sum(S-G)}{\overline{G}}\right) * 100$ (7)	$[-\infty, +\infty]$	0
Nash–Sutcliffe efficiency	NSE	$1 - \frac{\sum(G-S)^2}{\sum(G-\overline{G})^2}$ (8)	$[-\infty, 1]$	1

not detected by satellites, *F* number of precipitation events detected by satellites but not detected by rain gauges, *D* correct negative.

2.3.3 Assessment of the Rainfall Trends Using Various Satellite Products

The rainfall trends were assessed for the individual stations, using the mean monthly and annual rain gauge data versus the respective SPPs using the correlation coefficient (*r*) (Eq. 5) and per cent bias (Pbias) (Eq. 7), and using IDW interpolation in ArcMap 10.5.

3 Results

3.1 Evaluation of the Rainfall Estimate Performance of the Satellite Products

3.1.1 Daily Rainfall Comparisons

All the daily satellite precipitation products (SPPs) and rain gauge measurements showed medium agreement, i.e., the correlation coefficient r ranged from 0.37 to 0.52 and Nash–Sutcliffe model efficiency (NSE) coefficient showed negative values, i.e., − 1.57 to − 0.13 (Table 5). The summary of comparisons indicates that Climate Hazards Group Infrared Precipitation with Station Data (CHIRPS 2.0) had a relatively high probability of detection (POD). In contrast, African Rainfall Climatology (ARC 2.0) and Tropical Rainfall Measuring Mission (TRMM) Multi-satellite Precipitation Analysis (TMPA-3B42 7.0) products scored comparatively low values for POD (Table 5). The CHIRPS 2.0 scored higher probability false alarm ratio (POFA) value, 0.37. The ability of all the SPPs to detect rainy days was better than random chance, as indicated by Heidke skill score (HSS) values greater than zero. All SPPs underestimated daily rainfall rates; higher rates of underestimation of rain also recorded higher values of root mean square error (RMSE). Overall, CHIRPS 2.0 was the best-performing product, followed by Tropical Applications of Meteorology using SATellite and ground-based observations (TAMSAT 3.1). The categorical statistical indices (POD, POFA, BID, and HSS) results were not considered at monthly and annual timescales because cumulative monthly and annually precipitation cloud does not reflect specific precipitation events detected by SPPs.

3.1.2 Monthly Rainfall Comparisons

Monthly rainfall comparisons reveal reliable agreement between the six SPPs and ground-based rain gauge measurements, with the NSE coefficient ranging from 0.36 to 0.49, and a strong correlation coefficient of $r \geq 0.66$ (TableTable ***6***). Based on the statistical analysis, TAMSAT 3.1 performed better in estimating the monthly rainfall in the region than the other SPPs; TAMSAT 3.1 produced the best value of NSE, 0.49 and the lowest RMSE, 47.1. All SPPs overestimated the rainfall amount, except the ARC 2.0 product; the highest percent bias (Pbias) value was produced by the Precipitation Estimation from Remote Sensing Information using artificial neural networks-Climate Data Record (PERSIANN-CDR), 48.88% (Table 6). The SPPs produced relatively strong correlation coefficients against rain gauge observations; the TAMSAT 3.1 scored the highest *r* value, 0.71.

3.1.3 Annual Comparisons of Rainfall Totals

Strong agreement between the six SPPs and rain gauge measurements was demonstrated by annual comparisons, producing NSE coefficients ranging from 0.19 to 0.61

Table 5. The point-to-pixel evaluation at a daily timescale using continuous and categorical statistical tools; probability of detection (POD), probability of false alarm (POFA), bias in detection (BID) and Heidke skill score (HSS), correlation coefficient (r), root mean square error (RMSE), per cent bias (Pbias), and Nash-Sutcliffe efficiency (NSE)

Dataset	POD	POFA	BID	HSS	r	RMSE (mm day^{-1})	Pbias (%)	NSE
TMPA-3B42 7.0	0.43	0.27	0.59	0.23	0.41	57.85	-15.45	-1.41
CHIRPS 2.0	0.53	0.37	0.91	0.23	0.44	45.51	-12.15	-0.58
ARC 2.0	0.45	0.33	0.68	0.2	0.37	59.51	-17.61	-1.57
GPMIMERG 6.0	0.46	0.29	0.65	0.23	0.4	57.53	-15.36	-1.23
PERSIANN-CDR	0.51	0.31	0.9	0.16	0.49	24.47	-6.53	-0.21
TAMSAT 3.1	0.48	0.28	0.98	0.24	0.52	31.34	-8.37	-0.13

Performance: Weakest Strongest

Table 6. The point-to-pixel evaluation at a monthly timescale using continuous statistical tools; correlation coefficient (r), root mean square error (RMSE), per cent bias (Pbias), and Nash-Sutcliffe efficiency (NSE)

Dataset	r	RMSE (mm month^{-1})	Pbias (%)	NSE
TMPA-3B42 7.0	0.71	52.73	15.34	0.36
CHIRPS 2.0	0.73	50.64	1.49	0.41
ARC 2.0	0.67	51.19	-20.25	0.4
GPMIMERG 6.0	0.72	51.49	18.01	0.39
PERSIANN-CDR	0.66	76.66	48.88	-0.35
TAMSAT 3.1	0.75	47.1	10.29	0.49
Performance: Weakest				Strongest

(Table 7), and reliable correlation coefficients (*r*) ranging from 0.58 to 0.81 (Table 7). The Integrated Multi-satellitE Retrievals for Global Precipitation Measurements (GPM) Final Run (GPMIMERG 6.0) produced a relatively high correlation value. Based on the statistical analysis, the results indicated that TAMSAT 3.1 performed better than the other SPPs products; TAMSAT 3.1 produced the best value for the NSE and RMSE (Table 7). All SPPs overestimated the rainfall amount, except the ARC 2.0 product which provided an underestimate. The highest Pbias values was by PERSIANN-CDR, 82.69%.

The spatial distribution of mean annual rainfall is shown in Fig. 2. Various rainfall spatial patterns were observed among the six SPPs, with a clear north–south gradient of decreasing rainfall amounts. The areas in the south and southwest receive more rainfall compared to regions in the north and northeast. Based on the TMPA-3B42 7.0 satellite data, the annual rainfall in North Darfur for 2000–2019 ranged from 817.26 to 254.23 mm yr^{-1}, with a standard deviation of 146.34 mm yr^{-1}. The CHIRPS 2.0 dataset showed mean annual rainfall ranging from 784.46 to 189.83 mm yr^{-1}, with a standard deviation of 169.34 mm yr^{-1}. The ARC2.0-based product showed mean annual rainfall between 671.91 and 142 mm yr^{-1}, with a standard deviation of 127.5 mm yr^{--1}. The mean annual rainfall estimated by ARC2.0 dataset is also lower compared to the other products.

3.2 Mean Monthly Rainfall Trends

Spatio-temporal variation in the mean monthly precipitation for the 11 rain gauge stations using the six SPPs are shown in Fig. 3. The SPPs estimated the trends in rainfall for the rainy season, i.e., from May to October, with peak rainfall occurring during August and September (Fig. 3). All SPPs show that, comparatively, Kabkabiya, Saraf Omra, and Kutum, located in the Marra Mountains, receive more rainfall. As indicated by the SPPs, Kabkabiya, at an elevation of 1120 m, receives a monthly rainfall range 2.2–295.9 mm, while Saraf Omra, at an elevation of 1105 m, receives 2–380.5 mm. Kutum area at an elevation of 1160 m north of Marra mountains ranges 1.5–170.9 mm. Mellit and El Malha areas at lower elevation, recorded 1–119.7 mm and 3–129.2 mm, respectively.

TMPA-3B42 7.0 and CHIRPS 2.0 in Al Fashir (Table 8 and Fig. 4) recorded the highest correlation values. Al Liait recorded the lowest correlation values. The highest overestimated trends in rainfall were by PERSIANN-CDR), while the most underestimated trends in rainfall were by ARC 2.0.

Table 7. The point-to-pixel evaluation at an annual timescale using continuous statistical tools; correlation coefficient (r), root mean square error (RMSE), per cent bias (Pbias), and Nash-Sutcliffe efficiency (NSE)

Dataset	r	RMSE (mm annual^{-1})	Pbias (%)	NSE
TMPA-3B42 7.0	0.8	110.2	21.33	0.5
CHIRPS 2.0	0.78	112.4	22.85	0.39
ARC 2.0	0.76	89.8	-16.9	0.35
GPMIMERG 6.0	0.81	100.4	10.19	0.19
PERSIANN-CDR	0.58	235.2	82.69	-0.57
TAMSAT 3.1	0.71	8.7	14.98	0.61
Performance: Weakest				Strongest

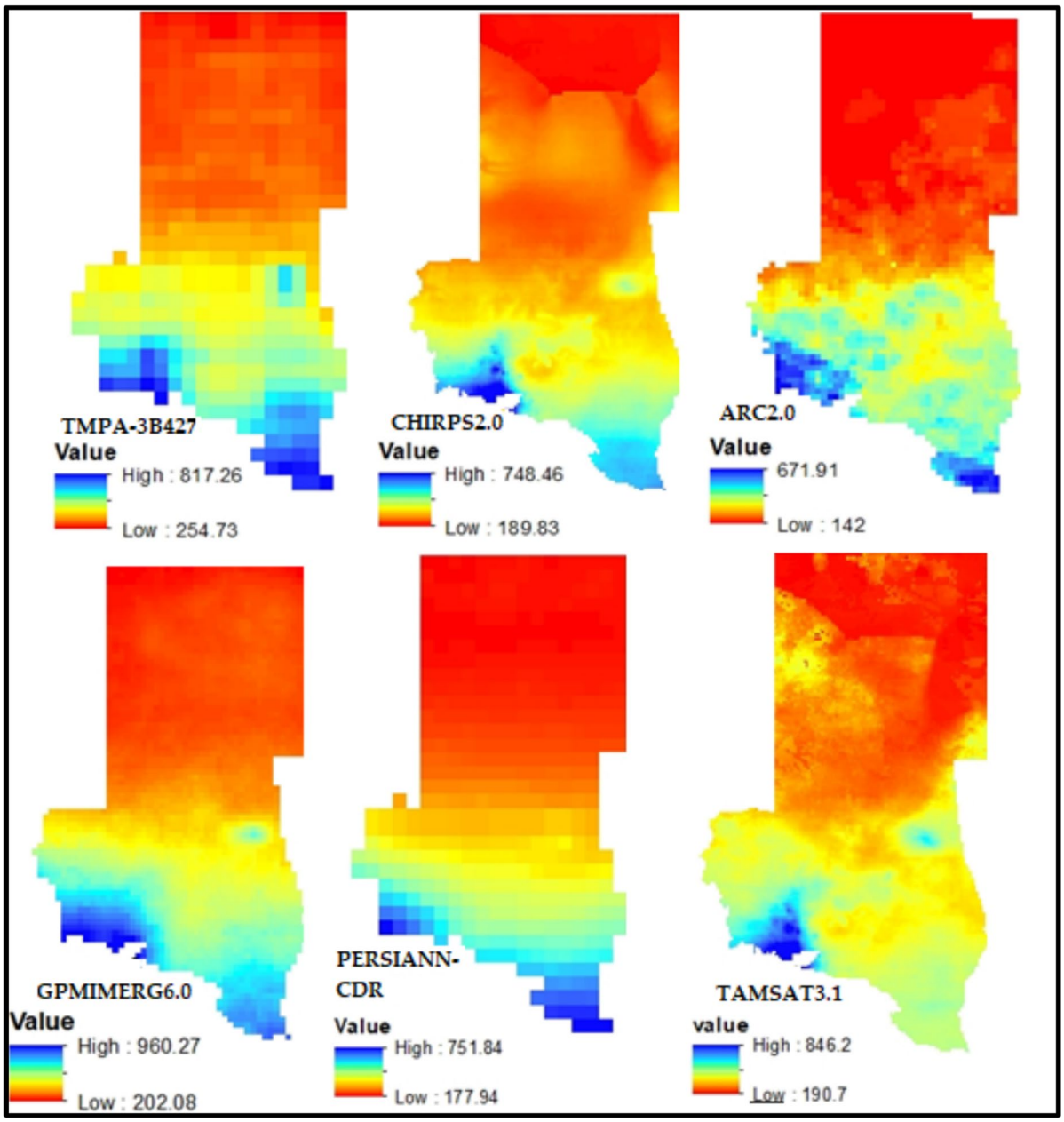


Fig. 2 Spatial distribution of mean annual rainfall over North Darfur from six satellites rainfall estimates for the periods 2000–2019

3.3 Mean Annual Rainfall Trends

Spatio-temporal variation in the mean annual precipitation for the 11 rain gauge stations using the six SPPs is shown in Fig. 5. El Malha receives between 26 and 542.1 mm, while Mellit receives 92–545 mm. The wetter Kabkabiya, Saraf Omra, and Kutum areas recorded rainfall in the range 206–1113 mm, 188–1205 mm, and 103–551 mm, respectively.

The highest correlation values were in El Malha by GPMIMERG 6.0 and ARC 2.0 (Table 9 and Fig. 6). Others were TAMSAT 3.1 in Kutum and PERSIANN-CDR in Kuma, Kutum and Kabkabiya. The PERSIANN-CDR reported the most overestimated trends in rainfall, while the most underestimated trends in rainfall were by CHIRPS 2.0. Generally, the best performing SPPs were TMPA-3B42 7.0 (Al Fashir, Dar ES Salam) and TAMSAT 3.1 (Kabkabiya, Saraf Omra).

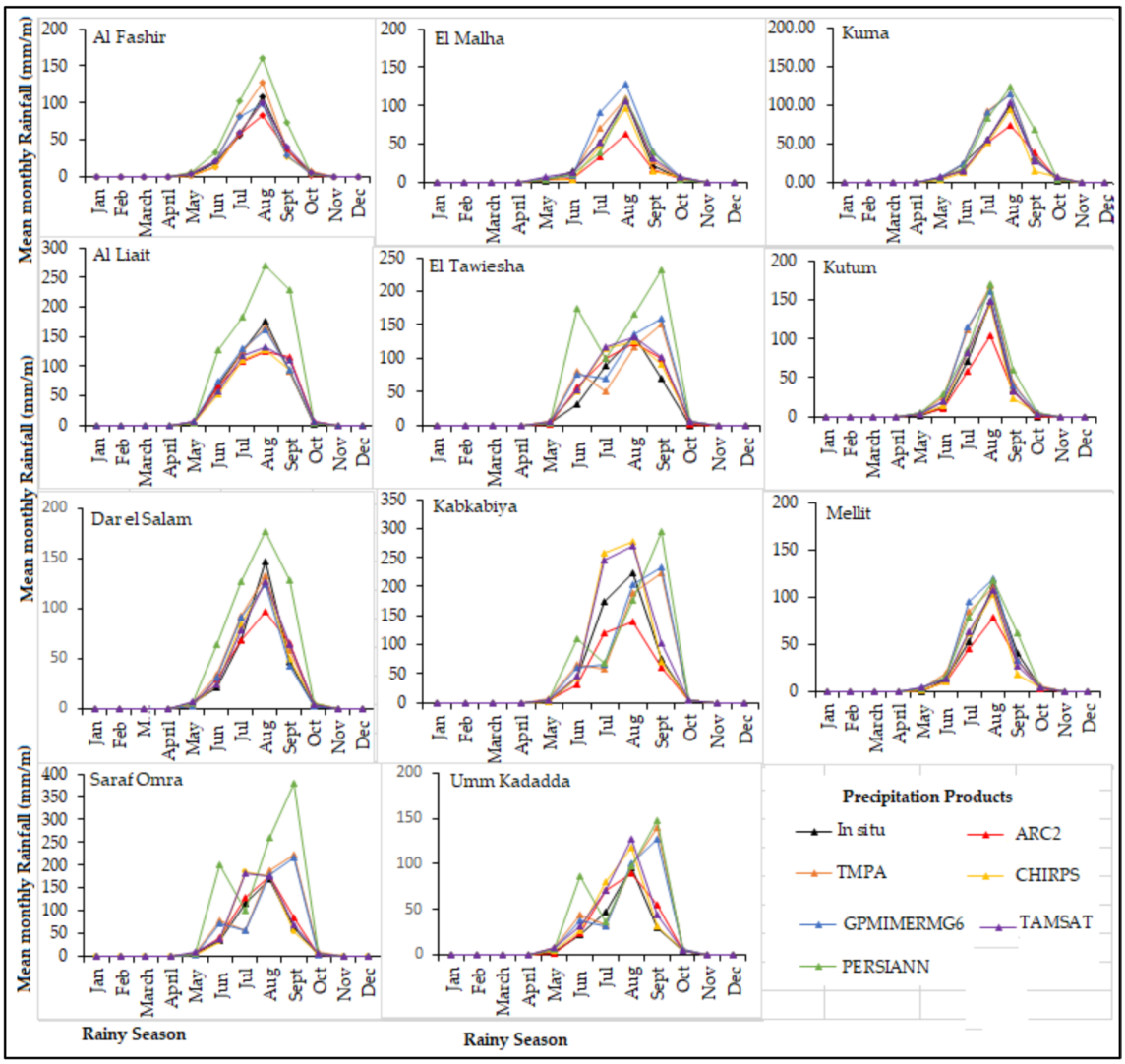


Fig. 3 Comparison of rain gauge observations based on monthly rainfall trends for 11 stations over North Darfur State and six-satellite precipitation products over the 20-year study period (2000–2019)

4 Discussion

Rainfall in Africa is challenging to estimate accurately because it is majorly a result of convective rainstorms, which are very localized spatially and temporally. Rainfall in Sudan is mainly regulated by the seasonal movement of the Inter-Tropical Convergence Zone (ITCZ). Therefore, the rainfall is convective in nature, derived from showers and thunderstorms. The rainfall depicts an extreme spatial variation which the existing rain gauge network cannot monitor effectively. In fact, it is argued that no conceivable rain gauge network would be adequate for the country. The reliability and applicability of the current satellite precipitation products (SPPs) against rain gauge observations across North Darfur State of Sudan was evaluated for a 20-year study period, i.e., 2000–2019. The SPPs were the Tropical Rainfall Measuring Mission (TRMM) Multi-satellite Precipitation Analysis (TMPA-3B42 7.0), African Rainfall Climatology Version 2 (ARC 2.0), Climate Hazards Group Infrared Precipitation with Station Data (CHIRPS 2.0), Integrated Multi-satellitE Retrievals for Global Precipitation Measurements (GPM) Final Run v 6 (GPMIMERG 6.0), Precipitation Estimation from Remote Sensing Information using artificial neural networks-Climate Data Record (PERSIANN-CDR), and the Tropical Applications of Meteorology using SATellite and ground-based observations (TAMSAT 3.1). The satellite-based rainfall estimation was assessed at daily, monthly, and annual timescales using point-to-pixel-based pairwise statistics.

Table 8 The Performance of six SPPs in estimating rainfall trends on a monthly timescale at 11 stations, using correlation coefficient (*r*) and per cent bias (Pbias %)

Stations	Statistic	TMPA-3B427.0	CHIRPS 2.0	ARC 2.0	GPMIMERG 6.0	PERSIANN-CDR	TAMSAT 3.1
Al Fashir	*r*	0.83	0.84	0.61	0.80	0.80	0.72
	Pbias	24.91	− 10.23	− 19.72	5.56	67.57	3.62
Al Liait	*r*	0.48	0.41	0.25	0.42	0.20	0.48
	Pbias	− 17.78	− 13.79	0.05	70.88	− 9.39	− 3.36
Dar El Salam	*r*	0.61	0.62	0.56	0.59	0.45	0.72
	Pbias	15.19	1.99	− 6.96	4.68	72.00	8.17
El Malha	*r*	0.68	0.65	0.71	0.71	0.64	0.64
	Pbias	4.19	− 20.84	− 43.36	28.49	− 4.58	7.50
El Tawiesha	*r*	0.47	0.65	0.43	0.53	0.53	0.66
	Pbias	17.68	11.16	9.91	29.21	85.50	17.41
Kabkabiya	*r*	0.54	0.71	0.74	0.54	0.55	0.53
	Pbias	0.55	23.57	− 34.98	5.67	16.10	28.46
Kuma	*r*	0.56	0.61	0.44	0.57	0.55	0.61
	Pbias	− 15.65	− 14.13	27.71	37.49	− 2.47	29.27
Kutum	*r*	0.77	0.79	0.79	0.70	0.67	0.67
	Pbias	29.53	− 1.92	− 24.32	24.89	21.77	5.25
Mellit	*r*	0.66	0.70	0.69	0.64	0.61	0.61
	Pbias	14.59	− 10.77	− 24.68	21.38	25.45	− 1.94
Saraf Omra	*r*	0.50	0.70	0.68	0.39	0.46	0.72
	Pbias	20.90	14.25	42.32	143.12	27.26	49.51
Umm Kadadda	*r*	0.61	0.41	0.44	0.55	0.57	0.60
	Pbias	59.96	26.08	16.65	50.98	76.68	40.04

4.1 Validation of Satellite Precipitation Products at Daily Timescale

Although CHIRPS 2.0 recorded the highest probability of detection (POD), the probability of false alarm (POFA) was also the highest (Table 5). To the contrary, the TMPA-3B42 7.0 performed poorly—it only detected 43% of the observed rainfall events in the study area, although it reported the lowest POFA and bias in detection (BID). The PERSIANN-CDR reported the lowest root mean square error (RMSE) and percent bias (Pbias). Daily satellite rainfall had a low correlation (*r*) with the rain gauge data—the TAMSAT 3.1 recorded the highest correlation value, 0.53. The weak agreement between the SPPs and rain gauge observations is in line with Usman et al. [23] and Dembélé and Zwart [32] in the Sudano Sahelian zone of Nigeria and Burkina Faso, respectively—and that CHIRPS 2.0 was the product most capable of detecting rainy days. The subpar performance of the rainfall products can be primarily attributed to errors in satellite models when predicting the accumulation and distribution of rainfall [9, 32]. Another reason could be the presence of a high variance and lack of dynamic range in daily rainfall estimates [64]. The POD metric indicates that SPPs fail to identify precipitation events with short durations. Rainfall events in the study area are spatially and temporally discontinuous, and the duration of rainfall may not last for long; therefore, satellite sensors may not capture the rainfall events [65]. Another source of error is the presence of the Marrah highlands—the magnitude of rainfall is underestimated because satellite estimates normally miss precipitation that is enhanced by flow lifting over mountains [66].

4.2 Validation of Satellite Precipitation Products at Monthly Timescales

Overall, all SPPs relatively correlated well with rain gauge observations—as the time scale increases, the performance of SPPs improves significantly [2, 6, 67, 68]. The TAMSAT 3.1 showed the best correlation with rain gauge observations (Table Table 6). The best performance in RMSE was the TAMSAT, while the CHIRPS 2.0 recorded the lowest overestimation of monthly rainfall. The PERSIANN-CDR was the worst because it reported the lowest correlation coefficient, the highest RMSE, and the highest Pbias. Also, Gadouali and Messouli [69] in Morocco and Dembélé and Zwart [32] in Burkina Faso reported PERSIANN-CDR as the worst at detecting monthly rainfall events. The poor performance can be attributed to cloud-top infrared (IR) observations [70]. The only underestimation of rainfall was

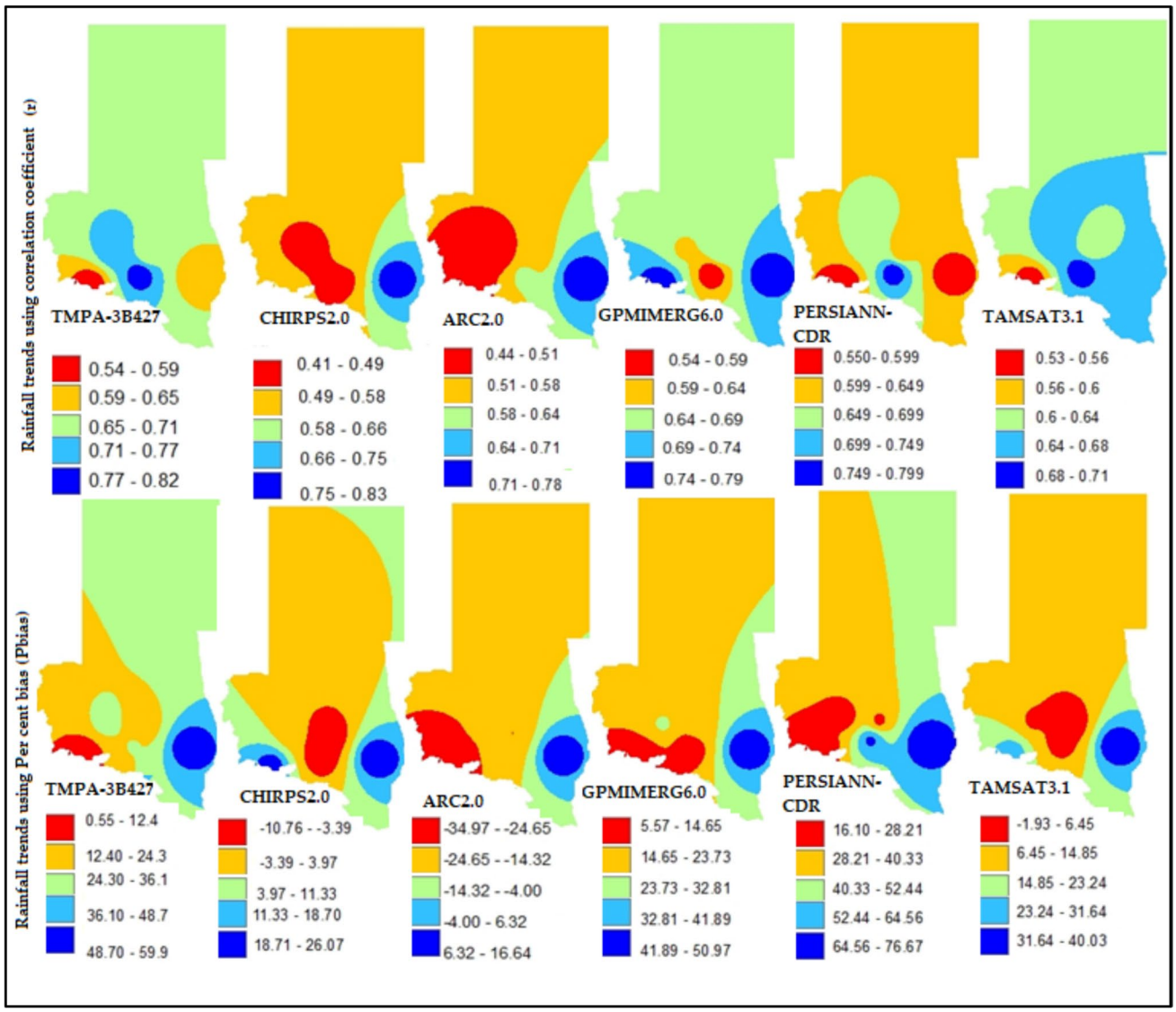


Fig. 4 Spatial plots of six SPPs estimating rainfall trends on a monthly timescale at 11 stations, using the correlation coefficient (*r*) and per cent bias (Pbias %)

from ARC 2.0, which is in agreement with Ayehu et al. [6]. The other five SPPs overestimated rainfall—Wedajo et al. [2] and Girma [36] reported overestimations of rainfall data from the TMPA-3B42 7.0, CHIRPS 2.0 and GPMIMERG 6.0, and TAMSAT 3.1, respectively. Gebremicael et al. [21] found that the CHIRPS 2.0 and TMPA-3B42 7.0 products underestimated rainfall in northern Ethiopia—the inconsistency with the current study may be due to differences in topography and/or climate conditions. Satellite precipitation products (SPPs) are known for overestimation of rainfall in arid and semiarid areas and underestimation in humid areas [71]. The overestimations are due to the fact that raindrops might evaporate before striking the surface [72], and the underestimation over higher altitude is due to strong scattering of the microwave (MW) signal by mountains [51] and misses the discrimination of warm clouds by IR sensors commonly found on the tops of mountainous regions [73]. Also, during the rainy season, satellite sensors have limited capability in detecting rainfall events because of non-raining clouds that could produce brief localized showers [74]. As well, intense rainfall can cause radar signals to attenuate, leading to inaccurate measurements [75].

Generally, the TAMSAT 3.1 and CHIRPS 2.0 performed better, and the PERSIANN-CDR performed poorly in all indices—this is consistent with Ageet et al. [18], Girma [36], Fenta et al. [76], Basheer and Elagib [77], and Dinku et al. [67]. The TAMSAT's primary benefit is that it employs local calibration datasets, where the temperature threshold and regression parameters are geographically and temporally variable [67]. The strong performance of CHIRPS 2.0 in

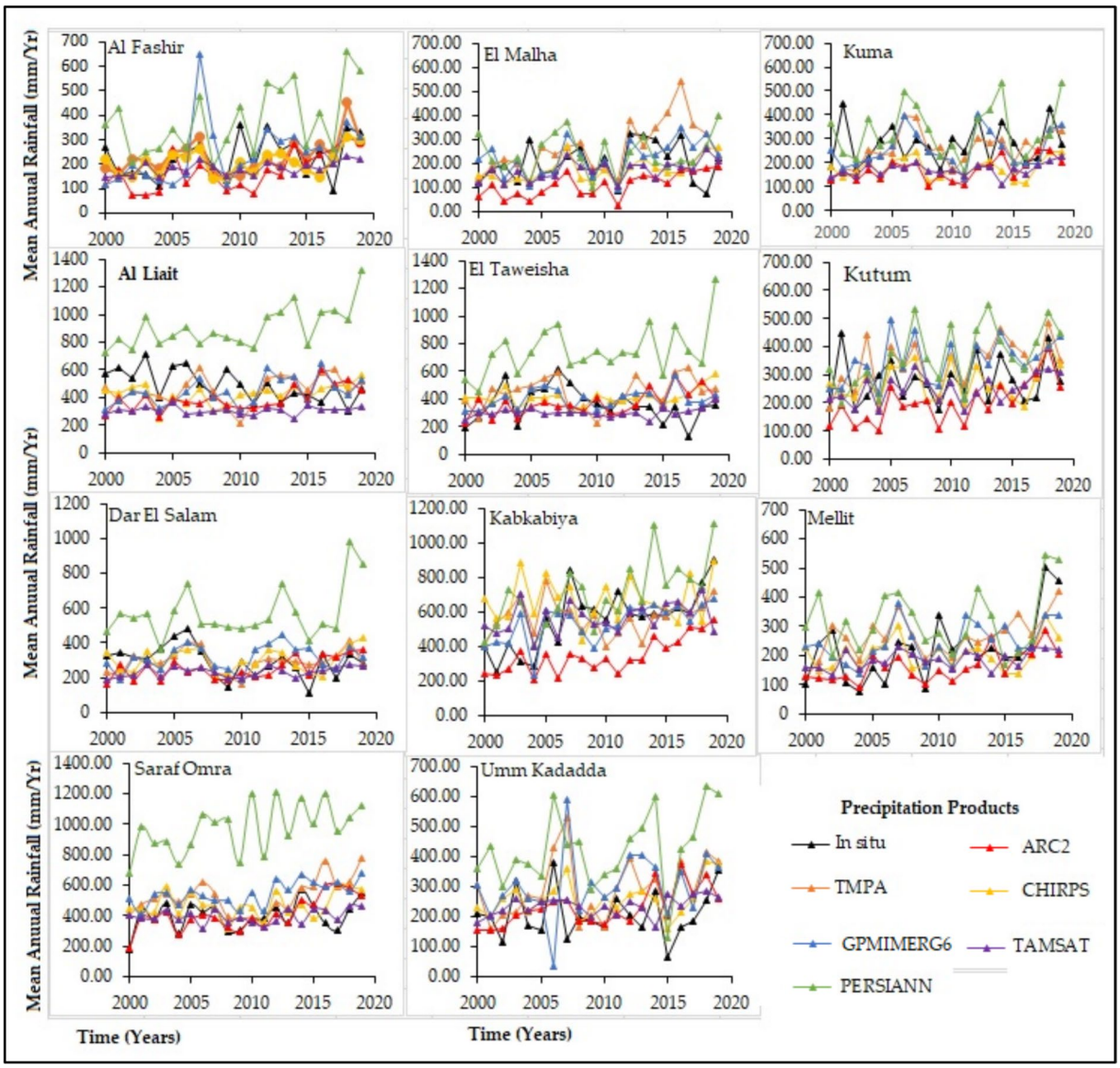


Fig. 5 Comparison of rain gauge observations based on annual rainfall trends in 11 stations over North Darfur State and six SPPs over the 20-year study period (2000–2019)

this study is in line with its high temporal and spatial resolution, capacity to integrate satellite data, and ability to gauge and reanalyze outputs [53]. The use of CHPClim, a gauge-satellite climatological tool, also offsets bias.

4.3 Validation of Satellite Precipitation Products at Annual Timescales

The GPMIMERG 6.0 and TMPA-3B42 7.0 were the highest correlated SPPs with rain gauge measurements (Table 7). The PERSIANN-CDR performed dismally, i.e., it recorded the lowest correlation coefficient, the worst RMSE, the highest overestimation of rainfall, and a negative Nash-Sutcliffe Efficiency (NSE). The TAMSAT 3.1 reported the least RMSE. Only ARC 2.0 underestimated annual rainfall, while the rest of the SPPs overestimated rainfall in the range. The TAMSAT 3.1 recorded the highest NSE value—higher values suggest a better agreement between rain gauge measurements and satellite estimates [62]. Overall, TAMSAT 3.1 performed better and the PERSIANN-CDR performed poorly in all indices. These results are in line with prior research on the Sudanese Blue Nile basin [35] and the East African Sio-Malaba-Malakisi River basin [13, 78]. However, a study carried out in Ethiopia's Upper Blue Nile basin contradicted the superiority of TAMSAT 3.1 at annual timescales [34]. The underperformance of the PERSIANN-CDR in capturing rainfall variability amounts is also consistent with studies conducted in East Africa [65] and northern

Table 9 The rainfall trends for the 20-year study period (2000–2019) were assessed at the annual timescale for six SPPS at 11 stations using the correlation coefficient (*r*) and per cent bias (Pbias %)

Stations	Statistic/products	TMPA-3B42 7.0	CHIRPS 2.0	ARC 2.0	GPMIMERG 6.0	PERSIANN-CDR	TAMSAT 3.1
Al Fashir	*r*	0.47	0.57	0.66	0.36	0.67	0.46
	Pbias	0.79	−24.26	−9.45	−16.26	65.96	−20.22
Al Liait	*r*	0.22	0.38	0.46	0.55	0.66	0.34
	Pbias	−6.37	−13.09	−20.22	−10.03	83.53	−37.56
Dar El Salam	r	0.43	0.51	0.39	0.17	0.47	0.46
	Pbias	−1.64	2.45	−13.79	7.22	92.38	−21.26
El Malha	*r*	0.42	0.34	0.82	0.83	0.37	0.52
	Pbias	29.50	−15.47	−44.78	6.97	12.97	−15.97
El Tawiesha	*r*	0.41	0.22	0.43	0.42	0.64	0.36
	Pbias	21.54	14.30	1.72	10.25	106.48	−16.81
Kabkabiya	*r*	0.23	0.46	0.56	0.70	0.72	0.25
	Pbias	23.25	−38.37	−3.59	25.58	1.12	1.30
Kuma	*r*	0.14	0.57	0.54	0.44	0.76	0.25
	Pbias	−7.25	−35.51	−38.05	−6.63	18.67	−37.98
Kutum	*r*	0.50	0.57	0.56	0.61	0.72	0.74
	Pbias	20.87	−0.96	−27.45	25.11	32.83	9.99
Mellit	*r*	0.61	0.44	0.58	0.57	0.61	0.43
	Pbias	19.08	−8.07	−26.94	11.15	42.91	−16.70
Saraf Omra	*r*	0.51	0.40	0.51	0.62	0.63	0.28
	Pbias	31.81	19.48	3.03	37.85	161.07	−0.90
Umm Kadadda	*r*	0.25	0.63	0.38	0.44	0.46	0.21
	Pbias	44.79	24.72	10.07	53.00	103.54	12.45

Egypt [79, 80]. The PERSIANN-CDR is calibrated based on Global Precipitation Climatology Project (GPCP) [81]; however, this does not guarantee improved performance in the study area. The performance of GPMIMERG 6.0 in rainfall estimations is superior to that of ARC 2.0 and PERSIANN-CDR, as confirmed by Zhang et al. [82]. Owing to the dual and high-frequency channels, which improve the detection of light and solid precipitation, GPMIMERG 6.0 has a superior performance [55]. This can be explained by the greater efficiency of MW sensors—satellite products that use MW sensors to measure rainfall perform better than those that use IR sensors [83]. Generally, the IR sensor compared to passive/active MW can lead to high POFA, and low POD, especially in sub-tropics and semi-arid and arid regions [84].

4.4 Station-wise Mean Monthly and Annual Rainfall Trends

In this study, the rate of rainfall is linearly related to altitude—comparatively, the area located in the south, around the Marrah Mountains, roughly receives more rainfall compared to the north, the low land. Station-wise monthly rainfall trends showed that not all SPPs followed similar pattern as the rain gauge data—notable was the PERSIANN-CDR and ARC2. The PERSIANN-CDR curve was conspicuously above the rain gauge and other SPPs curves in Al Fashir, Al Liait, and Dar el Salam. Severally, the PERSIANN-CDR curve exhibited a bimodal distribution, e.g., El Tawiesha, Kabkabiya, Saraf Omra, and Umm Kadadda, while the rain gauge curve showed only a single peak. Only in El Malha and Kutum stations, the PERSIANN-CDR closely followed the rain gauge curve. The ARC 2.0 curve was mostly below the rain gauge and other SPPs curves—only in Saraf Omra that the ARC 2.0 curve was almost the same as the rain gauge curve. The TAMSAT 3.1 and CHIRPS 2.0 closely followed the rain gauge curve pattern. The PERSIANN-CDR remains the worst at station-wise level with relatively low correlation coefficient compared to other SPPs. The TAMSAT 3.1 and CHIRPS 2.0 were better performers, with higher correlation coefficients. Compared to station-wise mean monthly rainfall trend, station-wise mean annual rainfall trends are different. The PERSIANN-CDR has relatively higher correlation coefficients compared to TAMSAT 3.1 and CHIRPS 2.0 in almost all rain gauge stations; although, the PERSIANN-CDR relatively overestimated the mean annual rainfall, compared to the other SPPs. Overall, the TAMSAT 3.1 and CHIRPS 2.0 were the best performers. Generally, all SPPs revealed increasing trends.

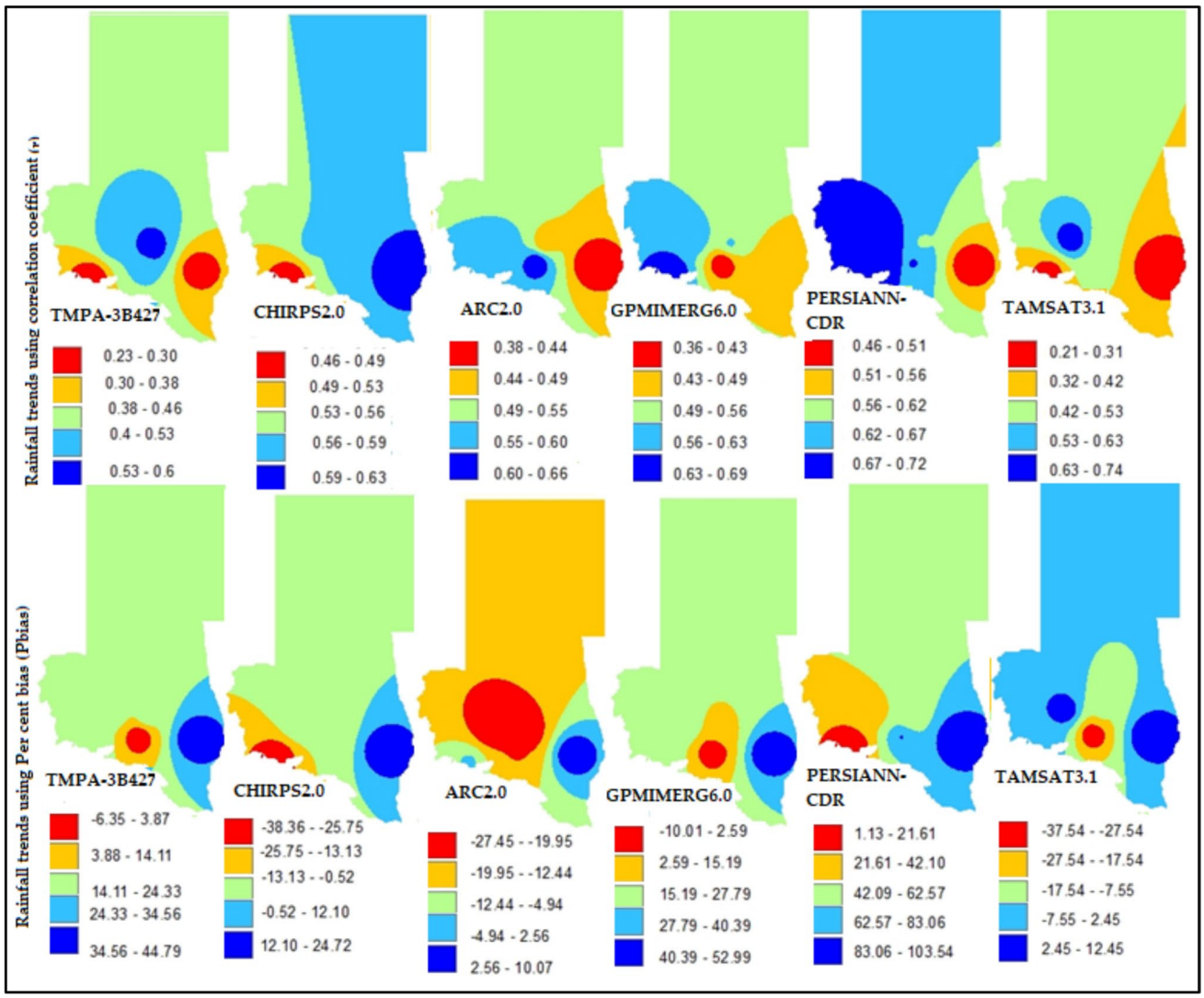


Fig. 6 Spatial plots of six SPPs estimating rainfall trends on an annual timescale at 11 stations, using the correlation coefficient (r) and per cent bias (Pbias %)

4.5 Study Limitations

This study used six SPPs and 11 rain gauge stations which are not spatially distributed in the climatic zones of North Darfur State. The variations in the quantity, quality, and distribution of rain gauge stations in the study area might have introduced errors that led to uncertainties in the performance of SPPs in capturing the spatio-temporal rainfall variability [64]. Also, the uncertainties attributed to errors in the retrieval algorithm, rain gauge measurement, and bias correction processes may render SPPs measurement of rainfall unreliable, because it may distort interpretation of the rainfall's behavior and simulation results by penetrating into other models such as the crop, hydrological, and meteorological models. The reliability of a particular rainfall dataset could vary with the temporal period of evaluation [64]. Another uncertainty may be associated with the point-to-pixel approach used that compared two datasets at different spatial scales [64]. Therefore, these errors cannot be ignored when using SPPs in various applications [48]. The errors could be the reason why several SPPs underestimated and/or overestimated rainfall in the study area. Therefore, comprehensive uncertainty characterization of satellite-derived rainfall products is vital. But the main limitation is the spatial and temporal resolutions of the data—investigating spatio-temporal variability of rainfall requires the use of precipitation datasets that have high spatial and temporal resolutions [85].

5 Conclusions

For climate studies and meteorological applications in data-poor regions of Africa, such as the Darfur region, satellite precipitation products (SPPs) represent an alternative source of rainfall data. The daily time intervals showed that there was a weaker agreement between SPPs and rain gauge measurements—the Climate Hazards Group Infrared Precipitation with Station Data (CHIRPS 2.0) was identified to be better in detecting rainy days. The results of the monthly and annual time scales showed that there was a stronger agreement between rain gauge observations and SPPs. Overall, the Tropical Applications of Meteorology using SATellite and ground-based observations (TAMSAT 3.1) and CHIRPS 2.0 were comparatively better—therefore, TAMSAT 3.1 and CHIRPS 2.0 could be reliable sources of rainfall data for stakeholders and researchers, in North Darfur. All SPPs exhibited errors in the continuous and categorical indices used—the SPPs indicated underestimations and overestimations in the analyses. Since the accuracy and reliability of satellite datasets is vital, future research should focus on more sophisticated algorithms and technological advancement that can provide near real-time data effective in improving the accuracy and reduce the uncertainties of estimated precipitation in data-scarce regions worldwide. Advanced SPPs data fusion techniques for infrared (IR) and microwave (MW) datasets should be explored.

Acknowledgements The authors acknowledge NASA, NOAA, the University of Reading, and the University of California for providing easy access to satellite-based rainfall products. We also would like to thank the North Darfur State Ministry of Agriculture for providing the rainfall data.

Author contributions M B. A. writing—original draft preparation; methodology; Conceptualisation; software; validation; formal analysis; investigation; resources; E. A. conception, confirmation, formal analysis, writing—review and editing, visualisation, supervision; K.A. A. and C.M.J. review, validation and editing. All authors have read and agreed to the published version of the manuscript.

Funding Open access funding provided by University of the Witwatersrand.

Data Availability No datasets were generated or analysed during the current study.

Declarations

Competing interests The authors declare no competing interests.

Open Access This article is licensed under a Creative Commons Attribution 4.0 International License, which permits use, sharing, adaptation, distribution and reproduction in any medium or format, as long as you give appropriate credit to the original author(s) and the source, provide a link to the Creative Commons licence, and indicate if changes were made. The images or other third party material in this article are included in the article's Creative Commons licence, unless indicated otherwise in a credit line to the material. If material is not included in the article's Creative Commons licence and your intended use is not permitted by statutory regulation or exceeds the permitted use, you will need to obtain permission directly from the copyright holder. To view a copy of this licence, visit http://creativecommons.org/licenses/by/4.0/.

References

1. Choubin B, Khalighi-Sigaroodi S, Mishra A, Goodarzi M, Shamshirband S, Ghaljaee E, Zhang F (2019) A novel bias correction framework of TMPA 3B42 daily precipitation data using similarity matrix/homogeneous conditions. Sci Total Environ 694:133680. https://doi.org/10.1016/j.scitotenv.2019.133680
2. Wedajo GK, Muleta MK, Awoke BG (2021) Performance evaluation of multiple satellite rainfall products for Dhidhessa River Basin (DRB), Ethiopia. Atmos Meas Tech 14:2299–2316. https://doi.org/10.5194/amt-2020-355
3. Duhan D, Pandey A (2013) Statistical analysis of long term spatial and temporal trends of precipitation during 1901–2002 at Madhya Pradesh, India. Atmos Res 122:136–149. https://doi.org/10.1016/j.atmosres.2012.10.010
4. RI Maidment Coauthors, 2017 A new, long-term daily satellite-based rainfall dataset for operational monitoring in Africa Scientific data 4 1 19 https://doi.org/10.1038/sdata.2017.63
5. Stillman S, Ninneman J, Zeng X, Franz T, Scott RL, Shuttleworth WJ, Cummins K (2014) Summer soil moisture spatiotemporal variability in southeastern Arizona. J Hydrometeorol 15:1473–1485. https://doi.org/10.1175/jhm-d-13-0173.1
6. Ayehu GT, Tadesse T, Gessesse B, Dinku T (2018) Validation of new satellite rainfall products over the Upper Blue Nile Basin, Ethiopia. Atmos Meas Tech 11:1921–1936. https://doi.org/10.5194/amt-2017-294
7. Brocca L, Coauthors (2016) Rainfall estimation by inverting SMOS soil moisture estimates: a comparison of different methods over Australia. J Geophys Res-Atmos 121 (12):062–012,079. https://doi.org/10.1002/2016JD025382
8. Asfaw A, Simane B, Hassen A, Bantider A (2018) Variability and time series trend analysis of rainfall and temperature in northcentral Ethiopia: a case study in Woleka sub-basin. Weather Clim Extremes 19:29–41. https://doi.org/10.1016/j.wace.2017.12.002
9. Zambrano-Bigiarini M, Nauditt A, Birkel C, Verbist K, Ribbe L (2017) Temporal and spatial evaluation of satellite-based rainfall estimates across the complex topographical and climatic gradients of Chile. J Hydrol Earth Syst Sci 21:1295–1320. https://doi.org/10.5194/hess-2016-453
10. Field CB, Barros VR (2014) Climate change 2014–impacts, adaptation and vulnerability: regional aspects. Cambridge University Press
11. Zakieldeen SA (2009) Adaptation to climate change: a vulnerability assessment for Sudan. Gatekeeper series/International Institute for Environment and Development. Sustain Agric Rural Livelihoods Programme 142.
12. Ibrahim FN (1984) Ecological imbalance in the Republic of the Sudan: with reference to desertification in Darfur.
13. AbdElhamid AM, Eltahan AM, Mohamed LM, Hamouda IA (2020) Assessment of the two satellite-based precipitation products TRMM and RFE rainfall records using ground based measurements. Alex Eng J 59:1049–1058. https://doi.org/10.1016/j.aej.2020.03.035
14. Osman YZ, Shamseldin AY (2002) Qualitative rainfall prediction models for central and southern Sudan using El Niño-Southern

Oscillation and Indian Ocean sea surface temperature indices. Int J Climatol Int J Climatol 22:1861–1878. https://doi.org/10.1002/joc.860
15. Elhag KM, Zhang W (2018) Monitoring and assessment of drought focused on its impact on sorghum yield over Sudan by using meteorological drought indices for the period (2001–2011). Remote Sens 10:1231. https://doi.org/10.3390/rs10081231
16. Kevane M, Gray L (2008) Darfur: rainfall and conflict. J Environ Res Lett 3:034006. https://doi.org/10.2139/ssrn.1147303
17. Paredes Trejo FJ, Alves Barbosa H, Peñaloza-Murillo MA, Moreno MA, Farias A (2016) Intercomparison of improved satellite rainfall estimation with CHIRPS gridded product and rain gauge data over Venezuela. Atmosfera 29:323–342. https://doi.org/10.20937/atm.2016.29.04.04
18. Ageet S, Fink AH, Maranan M, Diem JE, Hartter J, SsaliAgeet S, Fink AH, Maranan M, Diem JE, Hartter J, Ayabagabo SAL, PP (2022) Validation of satellite rainfall estimates over equatorial East Africa. J Hydrometeorol 23:129–151. https://doi.org/10.1175/jhm-d-21-0145.1
19. Kidd C, Huffman G (2011) Global precipitation measurement. Meteorol Appl 18:334–353. https://doi.org/10.1002/met.284
20. Toté C, Patricio D, Boogaard H, Van der Wijngaart R, Tarnavsky E, Funk C (2015) Evaluation of satellite rainfall estimates for drought and flood monitoring in Mozambique. Remote Sens 7:1758–1776. https://doi.org/10.3390/rs70201758
21. Gebremichael M, Krajewski WF, Morrissey ML, Huffman GJ, Adler RF (2005) A detailed evaluation of GPCP 1 daily rainfall estimates over the Mississippi River Basin. J Appl Meteorol Climatol 44:665–681. https://doi.org/10.1175/jam2233.1
22. Di Paola F, Casella D, Dietrich S, Mugnai A, Ricciardelli E, Romano F, Sanò P (2012) Combined MW-IR Precipitation Evolving Technique (PET) of convective rain fields. Nat Hazards Earth Syst Sci 12:3557–3570. https://doi.org/10.5194/nhess-12-3557-2012
23. Usman M, Nichol JE, Ibrahim AT, Buba LF (2018) A spatio-temporal analysis of trends in rainfall from long term satellite rainfall products in the Sudano Sahelian zone of Nigeria. Agric For Meteorol 260:273–286. https://doi.org/10.1016/j.agrformet.2018.06.016
24. HuffmanCoauthors GJ (1997) The global precipitation climatology project (GPCP) combined precipitation dataset. B Am Meteorol Soc 78:5–20. https://doi.org/10.1175/1520-0477(1997)078%3c0005:tgpcpg%3e2.0.co;2
25. Xie P, Arkin PA (1998) Global monthly precipitation estimates from satellite-observed outgoing longwave radiation. J Clim 11:137–164. https://doi.org/10.1175/1520-0442(1998)011%3c0137:gmpefs%3e2.0.co;2
26. Boushaki FI, Hsu K-L, Sorooshian S, Park G-H, Mahani S, Shi W (2009) Bias adjustment of satellite precipitation estimation using ground-based measurement: a case study evaluation over the southwestern United States. J Hydrometeorol 10:1231–1242. https://doi.org/10.1175/2009JHM1099.1
27. Ebert EE, Janowiak JE, Kidd C (2007) Comparison of near-real-time precipitation estimates from satellite observations and numerical models. B Am Meteorol Soc 88:47. https://doi.org/10.1175/Bams-88-1-47
28. Katiraie-Boroujerdy P-S, Asanjan AA, Hsu K-l, Sorooshian S (2017) Intercomparison of PERSIANN-CDR and TRMM-3B42V7 precipitation estimates at monthly and daily time scales. Atmos Res 193:36–49. https://doi.org/10.1016/j.atmosres.2017.04.005
29. Sanogo S, Fink AH, Omotosho JA, Ba A, Redl R, Ermert V (2015) Spatio-temporal characteristics of the recent rainfall recovery in West Africa. Int J Climatol 35:4589–4605. https://doi.org/10.1002/joc.4309
30. Dezfuli AK, Ichoku CM, Huffman GJ, Mohr KI, Selker JS, Van De Giesen N, Hochreutener R, Annor FO (2017) Validation of IMERG precipitation in Africa. J Hydrometeorol 18:2817–2825. https://doi.org/10.1175/jhm-d-17-0139.1
31. Bai J, Shi H, Yu Q, Xie Z, Li L, Luo G, Jin N, Li J (2019) Satellite-observed vegetation stability in response to changes in climate and total water storage in Central Asia. Sci Total Environ 659:862–871. https://doi.org/10.1016/j.scitotenv.2018.12.418
32. Dembélé M, Zwart SJ (2016) Evaluation and comparison of satellite-based rainfall products in Burkina Faso, West Africa. Int J Remote Sens 37:3995–4014. https://doi.org/10.1080/01431161.2016.1207258
33. Ayugi BO, Wen W ,Chepkemoi D (2016) Analysis of spatial and temporal patterns of rainfall variations over Kenya. Studies 6.
34. Bayissa Y, Tadesse T, Demisse G, Shiferaw A (2017) Evaluation of satellite-based rainfall estimates and application to monitor meteorological drought for the Upper Blue Nile Basin. Ethiopia Remote Sens 9:669. https://doi.org/10.3390/rs9070669
35. Ahmed AB, Elmagboul A, Desougi MA, Ali SAM ,Kodeal GAF (2020) Some soil physicochemical characteristics affected by land use change at El Salaam locality, South Darfur State, Sudan.
36. Girma D (2021) Evaluation and bias correction of tropical applications of meteorology using SATellite (TAMSAT) daily rainfall estimates over the data-scarce region of Southern Ethiopia J Civ Eng 121:2–7 https://doi.org/10.47363/jcert/2021(3)121
37. Lu X, Wang L, Pan M, Kaseke KF, Li B (2016) A multi-scale analysis of Namibian rainfall over the recent decade–comparing TMPA satellite estimates and ground observations. J Hydrol Reg Stud 8:59–68. https://doi.org/10.1016/j.ejrh.2016.07.003
38. Babaousmail H, Hou R, Ayugi B ,Gnitou GT (2019) Evaluation of satellite-based precipitation estimates over Algeria during (1998–2016) .J Atmos Sol Terr Phys 195:105139.https://doi.org/10.1016/j.jastp.2019.105139
39. Maidment R, Grimes DI, Allan RP, Greatrex H, Rojas O, Leo O (2013) Evaluation of satellite-based and model re-analysis rainfall estimates for Uganda. Meteorol Appl 20:308–317. https://doi.org/10.1002/met.1283
40. Osman A (2012) Agricultural change, land and violence: an examination of the region of Darfur, Sudan, PhD Dissertation, Food Policy and Applied Nutrition, Gerald J. and Dorothy R
41. Siddig K, Stepanyan D, Wiebelt M, Grethe H ,Zhu TJ (2020) Climate change and agriculture in the Sudan: impact pathways beyond changes in mean rainfall and temperature. J Ecol Econ 169:106566. https://doi.org/10.1016/j.ecolecon.2019.106566.
42. Brauch HG (2006) Desertification–a new security challenge for the Mediterranean? Policy agenda for recognising and coping with fatal outcomes of global environmental change and potentially violent societal consequences. Desertification in the Mediterranean Region. A Security Issue, Springer:11–85. https://doi.org/10.1007/1-4020-3760-0_02
43. Elagib NA, Al Zayed IS, Saad SAG, Mahmood MI, Basheer M, Fink AH (2021) Debilitating floods in the Sahel are becoming frequent. J Hydrol 599:126362. https://doi.org/10.1016/j.jhydrol.2021.126362
44. Osman AMK,Cohen MJ (2014) We no longer share the land: agricultural change, land, and violence in Darfur.
45. A Mohmmed ,Coauthors, 2018 Analysis of drought and vulnerability in the North Darfur region of Sudan Land Degrad Dev 29 4424 4438 https://doi.org/10.1002/ldr.3180
46. Siddig K (2010) Macroeconomy and agriculture in Sudan: analysis of trade policies, external shocks, and economic bans in a computable general equilibrium approach. Available at SSRN 1684084.

47. Young H, Osman AM, Aklilu Y, Dale R, Badri B, Fuddle A (2005) Darfur (2005) Livelihoods under siege. Feinstien International Famine Center, Tufts University, Medford, p 130
48. Taye M, Mengistu D, Sahlu D (2023) Performance evaluation of multiple satellite rainfall data sets in central highlands of Abbay Basin. Ethiopia Eur J Remote Sens 56:2233686. https://doi.org/10.1080/22797254.2023.2233686
49. Organization WM (2017) WMO guidelines on the calculation of climate normals. World Meteorological Organization Geneva, Switzerland.
50. Yong b, and coauthors, (2014) intercomparison of the version-6 and version-7 TMPA precipitation products over high and low latitudes basins with independent gauge networks: is the newer version better in both real-time and post-real-time analysis for water resources and hydrologic extremes? J Hydrol 508:77–87. https://doi.org/10.1016/j.jhydrol.2013.10.050
51. Huffman GJ, Coauthors, (2007) The TRMM multisatellite precipitation analysis (TMPA): quasi-global, multiyear, combined-sensor precipitation estimates at fine scales. J Hydrometeorol 8:38–55. https://doi.org/10.1175/jhm560.1
52. Novella NS, Thiaw WM (2013) African rainfall climatology version 2 for famine early warning systems. JAMC 52:588–606. https://doi.org/10.1175/jamc-d-11-0238.1
53. Funk C, Verdin A, Michaelsen J, Peterson P, Pedreros D, Husak G (2015) A global satellite-assisted precipitation climatology. Earth Syst Sci Data 7:275–287. https://doi.org/10.5194/essd-7-275-2015
54. O. S., Foelsche U, Kirchengast G, Fuchsberger J, Tan J, Petersen WA, (2017) Evaluation of GPM IMERG early, late, and final rainfall estimates using WegenerNet gauge data in southeastern Austria. J Hydrol Earth Syst Sci 21:6559–6572. https://doi.org/10.5194/hess-21-6559-2017
55. Huffman GJ, Bolvin DT, Braithwaite D, Hsu K, Joyce R, Xie P ,Yoo S-H (2015) NASA global precipitation measurement (GPM) integrated multi-satellite retrievals for GPM (IMERG). J ATBD 4. https://doi.org/10.1007/978-3-030-24568-9_19.
56. Ashouri H, Coauthors, (2015) PERSIANN-CDR: daily precipitation climate data record from multisatellite observations for hydrological and climate studies. B Am Meteorol Soc 96:69–83. https://doi.org/10.1175/bams-d-13-00068.1
57. Hsu KL, Gao XG, Sorooshian S, Gupta HV (1997) Precipitation estimation from remotely sensed information using artificial neural networks. J Appl Meteorol 36:1176–1190. https://doi.org/10.1175/1520-0450(1997)036%3c1176:pefrsi%3e2.0.co;2
58. Tarnavsky E, Coauthors, (2014) Extension of the TAMSAT satellite-based rainfall monitoring over Africa and from (1983) to present. ISO4 Standard. J Appl Meteorol Climatol 53:2805–2822. https://doi.org/10.1175/jamc-d-14-0016.1
59. Maidment RI, and Coauthors (2014) The 30 year TAMSAT African rainfall climatology and time series (TARCAT) data set. J Geophys Res Atmos 119:10,619–610,644. https://doi.org/10.1002/2014jd021927
60. Grimes D, Pardo-Iguzquiza E, Bonifacio R (1999) Optimal areal rainfall estimation using raingauges and satellite data. J hydrol 222:93–108. https://doi.org/10.1016/s0022-1694(99)00092-x
61. Diem JE, Hartter J, Ryan SJ, Palace MW (2014) Validation of satellite rainfall products for western Uganda. J Hydrometeorol 15:2030–2038. https://doi.org/10.1175/JHM-D-13-0193.1
62. Nash JE, Sutcliffe JV (1970) River flow forecasting through conceptual models part I—a discussion of principles. J hydrol 10:282–290. https://doi.org/10.1016/0022-1694(70)90255-6
63. Legates DR, McCabe GJ Jr (1999) Evaluating the use of "goodness-of-fit" measures in hydrologic and hydroclimatic model validation. Water Resour Res 35:233–241. https://doi.org/10.1029/1998wr900018
64. Mekonnen K, Coauthors, (2023) Accuracy of satellite and reanalysis rainfall estimates over Africa: a multi-scale assessment of eight products for continental applications. J Hydrol Reg Stud 49:101514. https://doi.org/10.1016/j.ejrh.2023.101514
65. Haile AT, Habib E, Rientjes T (2013) Evaluation of the climate prediction center (CPC) morphing technique (CMORPH) rainfall product on hourly time scales over the source of the Blue Nile River. J Hydrol Process 27:1829–1839. https://doi.org/10.1002/hyp.9330
66. Castro LM, Miranda M, Fernández B (2015) Evaluation of TRMM multi-satellite precipitation analysis (TMPA) in a mountainous region of the central Andes range with a Mediterranean climate. J Hydrol Res 46:89–105. https://doi.org/10.2166/nh.2013.096
67. Dinku T, Ceccato P, Grover-Kopec E, Lemma M, Connor SJ, Ropelewski CF (2007) Validation of satellite rainfall products over East Africa's complex topography. Int J Remote Sens 28:1503–1526. https://doi.org/10.1080/01431160600954688
68. Wu Y, Zhang Z, Huang Y, Jin Q, Chen X, Chang J (2019) Evaluation of the GPM IMERG v5 and TRMM 3B42 v7 precipitation products in the Yangtze River basin. China Water J 11:1459. https://doi.org/10.3390/w11071459
69. Gadouali F, Messouli M (2020) Evaluation of multiple satellite-derived rainfall products over Morocco. Int J Hydrol Sci Tec 10:72–89. https://doi.org/10.1504/Ijhst.2020.104988
70. Beck H, Van D, Levizzani V, Schellekens J, DG, Martens B, DE R (2017) MSWEP: 3-hourly 0.25° global gridded precipitation (1979–2014) by merging gauge, satellite, and reanalysis data. hydro Earth Syst Sci 21:589–615. https://doi.org/10.1175/bams-d-17-0138.1
71. Ibrahim AH, Molla DD ,Lohani TK (2022) Performance evaluation of satellite-based rainfall estimates for hydrological modeling over Bilate river basin, Ethiopia. World J Eng. https://doi.org/10.1108/wje-03-2022-0106
72. McCollum JR, Gruber A, Ba MB (2000) Discrepancy between gauges and satellite estimates of rainfall in equatorial Africa. J Appl Meteorol 39:666–679. https://doi.org/10.1175/1520-0450-39.5.666
73. Cavalcante RBL, Ferreira DBD, Pontes PRM, Tedeschi RG, da Costa CPW, de Souza EB (2020) Evaluation of extreme rainfall indices from CHIRPS precipitation estimates over the Brazilian Amazonia. Atmos Res 238:104879. https://doi.org/10.1016/j.atmosres.2020.104879
74. Su J, Lü H, Wang J, Sadeghi AM, Zhu Y (2017) Evaluating the applicability of four latest satellite–gauge combined precipitation estimates for extreme precipitation and streamflow predictions over the upper Yellow River basins in China. Remote Sens 9:1176. https://doi.org/10.3390/rs9111176
75. Cheema MJM, Bastiaanssen WG (2012) Local calibration of remotely sensed rainfall from the TRMM satellite for different periods and spatial scales in the Indus Basin. Int J Remote Sens 33:2603–2627. https://doi.org/10.1080/01431161.2011.617397
76. Fenta AA, Coauthors, (2018) Evaluation of satellite rainfall estimates over the Lake Tana basin at the source region of the Blue Nile River. Atmos Res 212:43–53. https://doi.org/10.1016/j.atmosres.2018.05.009
77. Basheer M, Elagib NA (2019) Performance of satellite-based and GPCC 7.0 rainfall products in an extremely data-scarce country in the Nile Basin. Atmos Res 215:128–140. https://doi.org/10.1016/j.atmosres.2018.08.028
78. Omonge P, Feigl M, Olang L, Schulz K ,Herrnegger M (2022) Evaluation of satellite precipitation products for water allocation studies in the Sio-Malaba-Malakisi River Basin of East Africa. J. Hydrol. Reg. Stud. 39:100983. https://doi.org/10.31223/x51c8j.
79. Kimani MW, Hoedjes JCB, Su ZB (2017) An assessment of satellite-derived rainfall products relative to ground observations over East Africa. Remote Sens 9:430. https://doi.org/10.3390/rs9050430

80. Roushdi M (2022) Spatio-Temporal Assessment of Satellite Estimates and Gauge-Based Rainfall Products in Northern Part of Egypt. J. Clim 10:134. https://doi.org/10.3390/cli10090134
81. Liu XM, Yang TT, Hsu KL, Liu CM, Sorooshian S (2017) Evaluating the streamflow simulation capability of PERSIANN-CDR daily rainfall products in two river basins on the Tibetan Plateau. J Hydrol Earth Syst Sci 21:169–181. https://doi.org/10.5194/hess-21-169-2017
82. Zhang Z, Tian J, Huang Y, Chen X, Chen S, Duan Z (2019) Hydrologic evaluation of TRMM and GPM IMERG satellite-based precipitation in a humid basin of China. Remote Sens 11:431. https://doi.org/10.3390/rs11040431
83. Bitew MM, Gebremichael M (2011) Assessment of satellite rainfall products for streamflow simulation in medium watersheds of the Ethiopian highlands. J Hydrol Earth Syst Sci 15:1147–1155. https://doi.org/10.5194/hess-15-1147-2011.doi:10.5194/hess-15-1147-2011
84. Kidd C,Levizzani V (2022) Satellite rainfall estimation. Rainfall, Elsevier 135–170. https://doi.org/10.1016/b978-0-12-822544-8.00005-6
85. Pierre C, Bergametti G, Marticorena B, Mougin E, Lebel T ,Ali A (2011) Pluriannual comparisons of satellite-based rainfall products over the Sahelian belt for seasonal vegetation modeling. J Geophys Res Atmos 116. https://doi.org/10.1029/2011jd016115

Publisher's Note Springer Nature remains neutral with regard to jurisdictional claims in published maps and institutional affiliations.